

Second occurrence of okayamalite, $\text{Ca}_2\text{SiB}_2\text{O}_7$: chemical and TEM characterization

F. OLMI,¹ C. VITI,² L. BINDI,³ P. BONAZZI,^{3,*} AND S. MENCHETTI³

¹CNR, Centro di Studio per la Minerogenesi e la Geochimica Applicata, Via La Pira 4, I-50121 Firenze, Italy

²Dipartimento di Scienze della Terra, Via Laterina 8, I-53100 Siena, Italy

³Dipartimento di Scienze della Terra, Via La Pira 4, I-50121 Firenze, Italy

ABSTRACT

Okayamalite, $\text{Ca}_2\text{SiB}_2\text{O}_7$, was identified in a skarn sample from the Arendal district, Sørlandet, Norway, associated with datolite, calcite, apophyllite, and chlorite. The chemical composition was determined by analyzing both heavy (Ca and Si) and light (B and O) elements using an electron microprobe: the empirical formula based on seven O atoms is $\text{Ca}_{1.96}\text{Si}_{0.97}\text{B}_{2.07}\text{O}_{7.00}$. TEM investigation revealed that okayamalite is intergrown on a fine scale with amorphous silica, giving rise to a complex interpenetrating structure at the scale of few hundreds angstroms. Okayamalite probably was formed by a desilication-dehydroxylation process of the associated datolite.

INTRODUCTION

Okayamalite, $\text{Ca}_2\text{SiB}_2\text{O}_7$, was first found at the Fuka Mine, Japan, in a vein-like skarn consisting mainly of vesuvianite, calcite, and wollastonite, closely associated with datolite and other undetermined borates (Matsubara et al. 1998). The chemical composition and powder X-ray diffraction (XRD) pattern of okayamalite closely resemble those of both the synthetic compound $\text{Ca}_2\text{SiB}_2\text{O}_7$ (Bauer 1962) and B-melilite obtained by heating datolite $\text{CaBSiO}_4(\text{OH})$ (Tarney et al. 1973; Kimata 1978). The structure of datolite consists of sheets of corner-linked SiO_4 and BO_3OH tetrahedra separated by sheets of Ca cations coordinated by 8 anions (Foit et al. 1973). On the whole, the structure resembles the atomic arrangement found in minerals of the melilite group (Smith 1953). It is not surprising, therefore, that the transformation of datolite to okayamalite shows a high degree of topotaxy (Tarney et al. 1973). For this reason, we investigated a number of datolite-bearing samples by means of optical and roentgenographic methods. This paper deals with the chemical and microtextural characterization of okayamalite found in a sample from Arendal, Norway.

OCCURRENCE AND SPECIMEN DESCRIPTION

Okayamalite was obtained from a skarn sample from the Arendal district, Sørlandet, Norway (Museum of Natural History of the University of Florence, catalog no. 2662/I). Arendal is a well-known mining district that has long been exploited for skarn-type iron ores. The skarn was formed by metasomatic processes in pre-Cambrian limestones, in association with orogenic intrusion of igneous rocks that range in composition from diorite to granite (Bugge 1940). The ore deposit consists mainly of magnetite, with a lesser amount of hematite. Skarn

minerals include: garnet, titanite, vesuvianite, epidote, zoisite, clinopyroxene, amphibole, rhodonite, phlogopite, biotite, datolite, serpentine, scapolite, analcime, and babingtonite (Bugge 1940).

Okayamalite occurs in a vein sample that consists mostly of large (up to 6 mm) euhedral crystals of datolite and, to a lesser extent, calcite, apophyllite, and a chlorite-group mineral. Okayamalite forms millimeter-sized aggregates that are translucent and milky white in color, often resembling prismatic single crystals. The aggregates typically occur in small interstices among the large crystals of datolite. No macroscopic evidence for the datolite-okayamalite reaction was observed. Selected grains were characterized by powder XRD methods using a Philips diffractometer with $\text{CoK}\alpha$ radiation. Table 1 reports the diffraction data of okayamalite from Arendal; the XRD patterns are similar to those given by Matsubara et al. (1998) for the holotype specimen. All reflections were indexed and unit-cell parameters were refined by means of least-squares methods [$a = 7.1343(3)$, $c = 4.8240(3)$ Å]. A broad feature observed approximately at 2θ ($\text{CoK}\alpha$) $\sim 25.9^\circ$ ($d \sim 4$ Å) may be due to an amorphous phase present in our sample. Its position is consistent with that of amorphous silica, as reported in Mozzi and Warren (1969). Accordingly, okayamalite is the only crystalline phase present in the powder studied.

CHEMICAL COMPOSITION

A fragment of okayamalite was analyzed by wavelength-dispersive methods (WDS) using a Jeol JXA-8600 electron microprobe. No elements with $Z > 9$, other than Si and Ca, were detected by a preliminary 300 s energy-dispersive scan. Boron and O contents of okayamalite were also determined with the electron microprobe. Particular care was given to problems concerning the acquisition of light-element data. Due to the almost perfect overlap of the first-order $\text{C}1\text{L}1$ and $\text{C}1\text{L}n$ lines with the $\text{BK}\alpha$ line, the absence of chlorine, already assumed

* E-mail: pbcry@steno.geo.unifi.it

TABLE 1. X-ray powder diffraction patterns for okayamalites

hkl	1			2		
	d_{calc} (Å)	d_{obs} (Å)	I/I_0	d_{calc} (Å)	d_{obs} (Å)	I/I_0
111	3.4865	3.490	45	3.479	3.479	40
210	3.1906	3.193	2	3.182	3.186	2
201	2.8682	2.870	50	2.862	2.862	55
211	2.6612	2.663	100	2.655	2.654	100
220	2.5224	2.524	5	2.516	2.518	2
002	2.4120	2.413	3	2.408	2.410	2
102	2.2850	2.286	5	2.281	2.283	7
310	2.2561	2.257	10	2.250	2.251	10
221	2.2352	2.236	15	2.230	2.231	15
112	2.1761	2.177	2			
301	2.1330	2.134	20	2.128	2.129	20
311	2.0436	2.044	5	2.039	2.039	5
320	1.9787	1.9791	1			
212	1.9241	1.9243	30	1.920	1.920	35
321	1.8307	1.8310	2	1.826	1.827	1
400	1.7836	1.7837	3	1.779	1.778	2
222	1.7433	1.7435	5	1.739	1.740	5
410	1.7303	1.7304	7	1.726	1.726	10
330	1.6816	1.6816	7	1.677	1.677	5
401	1.6729	1.6730	5	1.669	1.668	5
312	1.6477	1.6477	15	1.644	1.644	20
411	1.6287	1.6288	5	1.625	1.625	8
003	1.6080	1.6080	3	1.605	1.605	7
420	1.5953	1.5953	3			
331	1.5879	1.5878	5	1.584	1.584	7
113	1.5321	1.5320	3	1.529	1.529	2
322	1.5298	1.5298	1	1.526	1.526	2
203	1.4659	1.4659	2			
213	1.4359	1.4358	5	1.433	1.434	5
412	1.4060	1.4059	1	1.403	1.403	1
223	1.3559	1.3558	1	1.353	1.354	1
511	1.3438	1.3436	1			
422	1.3306	1.3304	1			
521	1.2775	1.2773	5	1.274	1.274	5

Notes: (1) = okayamalite from Arendal District, Sørlandet, Norway (this study; monochromatized $\text{CoK}\alpha$); unit-cell parameters: $a = 7.1343(3)$; $c = 4.8240(3)$ Å. (2) = okayamalite from Fuka Mine, Okayama Prefecture, Japan (Matsubara et al. 1998); unit-cell parameters: $a = 7.116(2)$; $c = 4.815(1)$ Å.

on the the basis of preliminary EDS analysis, was verified by WDS. The Ca and O peaks (2nd-order $\text{CaL}\alpha$ and $\text{CaL}\beta$ lines, and 3rd-order $\text{OK}\alpha$ line) interfering with the $\text{BK}\alpha$ line were cut off by choosing a narrow window in the pulse height analyzer configuration (McGee and Anovitz 1996). The positions of B and O were always repeaked on the analyzed sample (both standard and unknown) to compensate for peak shifts.

Analytical conditions were an accelerating voltage of 10kV and a beam current of 150 nA. The standards used were diopside for Ca and Si, quartz for O, and synthetic boron nitride for B. A specimen of datolite (Museum of Natural History of the University of Florence, catalog n. 77/I) was carbon-coated together with the okayamalite sample, and was analyzed to verify instrument parameters. Long counting times (the same times on peak and on background) were used to improve statistics: 30 s for O, 60 s for Ca, and 90 s for B and Si. To reduce the unavoidable electron-beam damage and contamination effects on the sample surface, a 20 μm spot size was used. The operating conditions yielded net-peak counting precision statistic better than 0.5% for O, Ca, and Si, and better than 2% for B. The raw data were reduced using the $\phi(\rho z)$ correction routine in the Tracor-Northern system of programs (Bastin et al. 1987).

The experimental results are given in Table 2. The compo-

sition of the okayamalite sample (column 1) differs from that expected for pure okayamalite (column 4), although the instrumental configuration was confirmed using the datolite specimen (columns 2 and 3). The composition obtained for the okayamalite specimen matches the calculated composition for a mixture of $\text{Ca}_2\text{SiB}_2\text{O}_7$ plus SiO_2 with a 1:1 molar ratio (column 5).

Chemical data thus indicate that okayamalite is intermixed with silica (amorphous, on the basis of XRD data), in an approximately 1:1 ratio. Several backscattered electron images and X-ray maps (both WDS and EDS), acquired with high spatial resolution and long acquisition times, failed to show the presence of two phases. The wide range (column 1, Table 2) in measured composition is probably due to local variations in the okayamalite-silica ratio. After correcting for 1 molar SiO_2 , the empirical chemical formula (based on seven O atoms) for the Arendal okayamalite is $\text{Ca}_{1.96}\text{Si}_{0.97}\text{B}_{2.07}\text{O}_{7.00}$.

TEM INVESTIGATION

To investigate the proposed intergrowth of okayamalite and amorphous silica, we investigated the okayamalite sample using transmission electron microscopy (TEM). The TEM studies were carried out using a Jeol JEM 2010, an accelerating voltage of 200 kV, a ultra-high resolution (UHR) pole piece, and a point-to-point resolution close to 1.9 Å (the electron probe can be focused down to 100 Å in diameter). The microscope is equipped with a semi-STEM system and an energy dispersive spectrometer (EDS-ISIS Oxford, superthin window).

A small amount of okayamalite (the same specimen used for the powder XRD study) was dispersed onto Cu mesh grids (300 mesh, 3 mm in diameter) that had been previously covered by a thin carbon layer (support film). The powdered grids were further coated by carbon.

The sample consists of a fine intergrowth of crystalline okayamalite and amorphous silica on a scale of a few hundred angstroms (Fig. 1), below the limit of optical and microprobe resolution. On the basis of TEM-EDS data and selected area electron diffraction (SAED) patterns, dark-contrast areas (labeled a in Fig. 1) have been identified as crystalline okayamalite. In contrast, the low-contrast homogeneous areas (labeled b in

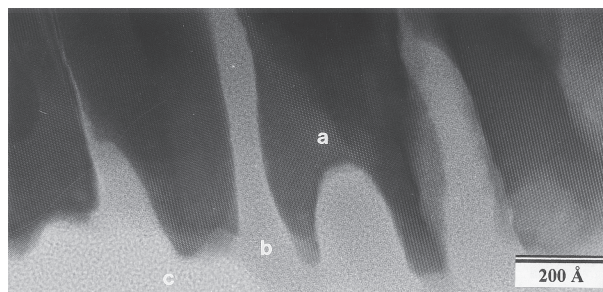


FIGURE 1. Intergrowth between crystalline okayamalite (a) and amorphous silica (b). Okayamalite here forms regular lamellae elongated along [001], typically 400 Å thick. The grainy area (c) corresponds to the graphite film.

TABLE 2. Experimental and theoretical chemical compositions for okayamalite and datolite

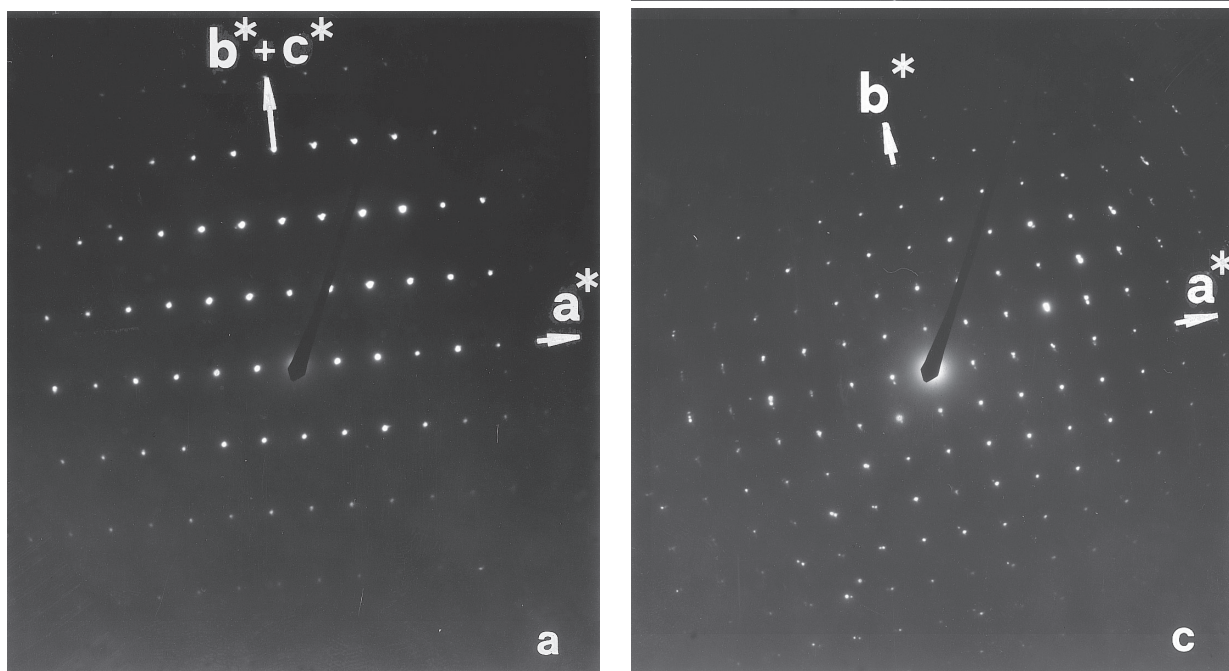
wt%	(1)	(2)	(3)	(4)	(5)			
Si	18.47	(17.90–19.10)	17.61	(17.49–17.78)	Si	17.56	11.61	18.60
Ca	26.31	(25.83–27.00)	24.76	(24.58–25.00)	Ca	25.05	33.14	26.55
B	7.49	(6.93–8.08)	7.11	(6.91–7.34)	B	6.76	8.93	7.16
O	48.03	(46.82–49.11)	50.32	(49.68–50.88)	O	50.00	46.32	47.69
					H	0.63	–	–
Total	100.30	99.80			Total	100.00	100.00	100.00

Note: Diffracting crystals used for the analysed elements were: N-STE ($2d = 100.4 \text{ \AA}$) for B, LDE1 ($2d = 60 \text{ \AA}$) for O, PET ($2d = 8.742 \text{ \AA}$) for Ca and Si. (1) = okayamalite + amorphous silica intergrowth from Arendal (see text): average of 19 spots (range in parenthesis). (2) = datolite: average of 11 spots (range in parenthesis). (3) = datolite: calculated atomic wt% for the ideal formula $\text{Ca}_2\text{B}_2\text{Si}_2\text{O}_8(\text{OH})_2$. (4) = okayamalite: calculated atomic wt% for the ideal formula $\text{Ca}_2\text{SiB}_2\text{O}_7 + \text{SiO}_2$.

Fig. 1) correspond to an amorphous phase (because no reflections are present in the corresponding diffraction patterns). The EDS data indicate that this amorphous phase corresponds to silica (only Si and O peaks in the EDS spectra). The amorphous silica is characterized by a grainy texture that can be easily distinguished from the grainy texture of the carbon film (labeled c in Fig.1).

Amorphous silica and crystalline okayamalite are present in roughly equivalent amounts, in agreement with the 1:1 ratio derived from WDS data. The intergrowth may appear as a quite regular sequence of amorphous layers and crystalline layers, typically 350–450 Å thick and elongated parallel to okayamalite [001], but in most cases it appears as a complex, interpenetrating random intergrowth, unrelated to the okayamalite crystallographic orientation. Okayamalite grains typically show irregular, lobate shapes, such that the intergrowth often resembles a “graphic texture”; the overall texture suggests crystallization under non-equilibrium conditions.

Different crystal orientations of okayamalite have been investigated. In particular, we collected electron diffraction patterns corresponding to the $[0\bar{1}1]$, $[010]$, and $[001]$ zone axis

**FIGURE 2.** SAED patterns of okayamalite. Electron beam along $[0\bar{1}1]$ (a), $[010]$ (b), and $[001]$ (c).

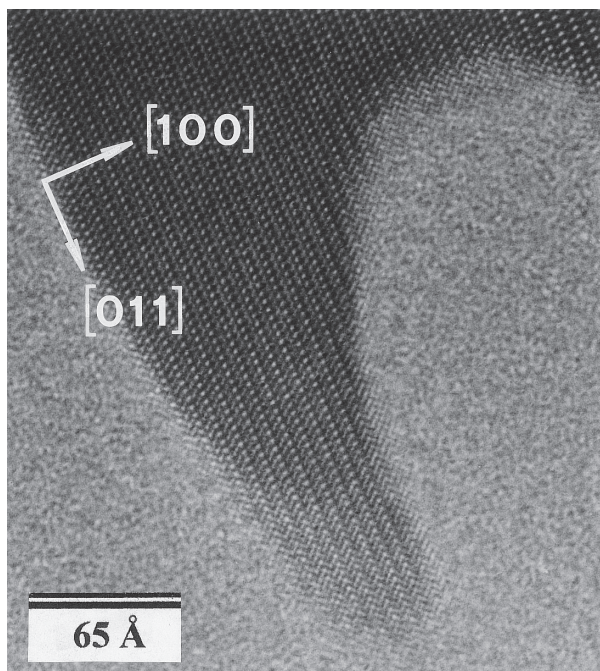


FIGURE 3. High-resolution image of okayamalite along the $[0\bar{1}1]$ zone axis. The arrows correspond to $[011]$ and $[100]$.

(Figs. 2a, 2b, and 2c, respectively). SAED patterns are characterized by sharp and intense reflections: no satellite spots were observed, thus precluding the presence of structural modulations. The extra reflections observed in Figures 2b and 2c, particularly in the outer zones of the reciprocal plane, are due to slight crystal misorientation. Figure 3 shows a high-resolution image of okayamalite corresponding to the $[0\bar{1}1]$ zone axis: the main d -spacings (measured along the two orthogonal arrows) correspond to $d_{100} = 7.12$ and $d_{011} = 3.99$ Å. The boundary between okayamalite and silica is sharp, even if irregular and unrelated to the okayamalite lattice planes. Note also that the structure of okayamalite is ordered and defect-free near the boundary with amorphous silica. No other phase associated with okayamalite and silica was found, in agreement with powder XRD diffraction pattern.

ORIGIN

The sample of okayamalite from Arendal consists of finely interpenetrated intergrowths of crystalline okayamalite and amorphous silica. Electron microprobe analysis indicates that the ratio of the two phases is approximately 1:1. Taking into account the experimental work by Tarney et al. (1973), it seems reasonable to assume that okayamalite was formed by a desilication-dehydroxylation process involving datolite. This reaction could occur under non-equilibrium conditions, as inferred from the irregular lobate-shaped texture and from the presence of metastable non-crystalline silica. However, the occurrence of unaltered euhedral crystals of datolite in the same sample casts some doubt on this genetic interpretation.

ACKNOWLEDGMENTS

Critical and careful reviews by two official referees and by Associate Editor Gilberto Artioli were greatly appreciated. The authors thank Joanne Krueger for reading the original manuscript. This work was funded by M.U.R.S.T., "cofinanziamento 1999," project "Transformations, reactions, ordering in minerals."

REFERENCES CITED

- Bastin, G.F., Loo, F.J.J.v., and Heijligers, H.J.M. (1987) Evaluation of the use of gaussian $\phi(\rho z)$ curves in quantitative electron probe microanalysis: a new optimization. Laboratory for Physical Chemistry, University of Technology, Eindhoven, The Netherlands.
- Bauer, H. (1962) Über Diadochie zwischen Aluminium und Bor in Gehlenit. *Neues Jahrbuch für Mineralogie Monatshefte*, 1962, 127–140.
- Bugge, J.A.W. (1940) Geological and petrological investigations in the Arendal district. *Norsk Geolog. Tidsskrift*, 20, 71–112.
- Foit, F.F. Jr., Phillips, M.W., and Gibbs, G.V. (1973) A refinement of the crystal structure of datolite, $\text{CaBSiO}_4(\text{OH})$. *American Mineralogist*, 58, 909–914.
- Kimata, M. (1978) Boron behavior in the thermal decomposition of datolite. *Neues Jahrbuch für Mineralogie Monatshefte*, 58–70.
- Matsubara, S., Miyawaki, R., Kato, A., Yokoyama, K., and Okamoto, A. (1998) Okayamalite, $\text{Ca}_2\text{B}_2\text{SiO}_8$, a new mineral, boron analogue of gehlenite. *Mineralogical Magazine*, 62, 703–706.
- McGee, J.J. and Anovitz, L.M. (1996) Electron probe microanalysis of geological material for boron. In *Mineralogical Society of America Reviews in Mineralogy*, 33, 771–788.
- Mozzi, R.L. and Warren, B.E. (1969) The structure of vitreous silica. *Journal of Applied Crystallography*, 2, 164–172.
- Smith, J.V. (1953) Reexamination of the crystal structure of melilite. *American Mineralogist*, 38, 643–661.
- Tarney, J., Nicol, A.W., and Marriner, G.F. (1973) The thermal transformation of datolite, $\text{CaBSiO}_4(\text{OH})$, to boron-melilite. *Mineralogical Magazine*, 39, 158–175.

MANUSCRIPT RECEIVED NOVEMBER 23, 1999

MANUSCRIPT ACCEPTED MAY 26, 2000

PAPER HANDLED BY GILBERTO ARTIOLI